Investigation of the effect of aging on wood hygroscopicity by 2D 1 H NMR relaxometry

Leila Rostom, Denis Courtier-Murias, Stéphane Rodts, Sabine Caré

Short title: **Wood aging observed by ^{1}H NMR relaxometry**

Investigation of the effect of aging on wood hygroscopicity by 2D ^{1}H NMR relaxometry

Leila ROSTOM[1], Denis COURTIER-MURIAS[1], Stéphane RODTS[1 †], Sabine CARE[1]*
[1] *Laboratoire Navier, UMR 8205, École des Ponts, IFSTTAR, CNRS, UPE, Champs-sur-Marne, France*
** Laboratoire Navier, Ecole des Ponts ParisTech, 6-8 avenue Blaise Pascal, Champs-sur-Marne, 77455 Marne-la-Vallée cedex 2, France*
sabine.care@ifsttar.fr

Abstract: 2D ^{1}H NMR relaxometry is increasingly used in the field of wood sciences due to its great potential in detecting and quantifying water states at the level of wood constituents. More precisely, in this study, this technique is used to investigate the changes induced by "natural" and "artificial" aging methods on modern and historical oak woods. Two bound water components are detected and present differences in terms of association to the different wood polymers in cell walls: one is more strongly associated to wood polymers than the other. The evolution of the two bound water types is discussed in regard to aging methods and is related to the structure of the cell wall, especially with the S2 layer and the evolution of wood chemical composition (cellulose, hemicelluloses and lignin). The evolution of hydric strains is discussed taking into account the effect of aging methods on the two bound water components too. The obtained results confirm the ability of 2D NMR relaxomety to evaluate the effect of aging at the molecular level and on hydric deformation. Furthermore, this method shows that it is possible to determine the moisture content of wood without the necessity to oven-dry the wood material.

Keywords: Aging, deformation, extractibles, hydric cycles, oak wood, thermal treatment, 2D NMR relaxometry

Introduction

The built heritage shows that wood makes it possible to design sustainable and healthy buildings (Epaud 2007, Obataya 2007, Froidevaux 2012). Wood, as an envelope or structural material, is a material of interest in the field of construction both for new buildings and for the question of renovation of old buildings (Froidevaux 2012). However, to estimate lifetimes or to propose methods of maintenance, it is necessary to continue the research efforts to understand the mechanisms of physical aging of wood and its hygro-mechanical properties at the scale of its constituents.

Aging is a complex phenomenon that modifies physical, chemical and mechanical properties of a polymeric based material, under the effect of its proper instability, environmental parameters or mechanical strains (Fayolle and Verdu 2005). As a natural and biodegradable resource, wood is mainly constituted of three biopolymers: cellulose, hemicellulose and lignin. These components can be vulnerable to environmental factors such as temperature, solar radiation, humidity, which can degrade the wood's polymeric structure. Studies have shown that the degradation due to aging mostly affect the hemicelluloses (which are the most vulnerable polymers), resulting in a better dimensional stability of the wood material (Kranitz 2014, Gauvin 2014). A decrease of cellulosic material as well as a slight decrease in lignin content are also observed in some historical woods (Kranitz et al. 2016). Heat treatments at high temperature show a common effect with natural aging on decreasing the Equilibrium Moisture Content (EMC), leading to an improved dimensional stability of wood and are usually considered as artificial aging. Numerous studies have been conducted to develop industrial processes varying in terms of temperature (generally at high temperature between 160°C and 280°C), duration and vector (gas, water vapour, oil…) (Tjeerdsma et al. 1998, Esteves and Pereira 2008, Wentzel et al. 2018) to improve the durability of timbers. The higher the temperature of treatment - and the longer the treatment time - the greater the dimensional stability of wood (Inari et al. 2009; Chaouch 2011; Endo et al. 2016). However, these treatments' intensity considerably weakens the mechanical properties of timbers (Hill 2006, Froidevaux 2012, Candelier 2016). Thus, thermal

treatments at lower temperature are proposed as a better alternative as they have a lower effect on the mechanical properties of timber. However, it remains unclear if the thermal treatments in presence or absence of humidity is the closest to a 'natural aging' effect. Some authors show that hydrothermal treatments in precise conditions of Relative humidity, Temperature and Pressure can mimic an aged wood in terms of its mechanical characteristics, colour change and decreased swelling rate (Froidevaux 2012, Gauvin 2015, Endo et al. 2016). Whereas in terms of dry heat treatments, it seems to be a better option than steam to reduce the hygroscopic capacity of wood, and improve its dimensional stability, with a minimum of thermal degradation (Obataya 2007, Matsuo et al. 2009, Sandberg and Navi 2013).

The wood hygroscopicity plays a major role on the dimensional stability and mechanical properties of wood. This improved dimensional stability may be explained by a decrease in adsorption sites in the polymers chains of the wood cell walls (Hill 2006, Froidevaux 2012, Murata et al. 2013). However, in Rautkari et al. 2013, a poor correlation between EMC, sorption sites accessibility and theoretical hydroxyl group content was found following a thermal treatment and therefore additional mechanisms should exercise control over the EMC. This shows that water interactions with wood (hygroscopicity and dimensional stability) are still not completely understood, which can be explained by the difficulty to characterize adsorbed water in wood. The use of proton Nuclear Magnetic Resonance (^{1}H NMR) relaxometry to detect bound water in the wood's cell walls is gaining popularity in the research field as it is a non-invasive method allowing to study the same material subjected to different loadings. Here, we investigate the state of water adsorbed on the wood's cell walls through ^{1}H low-field (LF) NMR relaxometry (Menon et al. 1987, Araujo et al. 1994, Labbé et al. 2002, Fredriksson and Garbrecht Thygesen 2017, Beck et al. 2018). Recent studies (Cox et al. 2010, Bonnet et al. 2017) have used two-dimensional (2D) T_1-T_2 correlation spectra, allowing to differentiate two different types of bound water, which have been assigned to water adsorbed to different wood polymers in the hygroscopic range (Bonnet et al. 2017). So far, this technique is the

sole tool capable to observe two different types of bound water in wood. Thus, 2D ^{1}H NMR correlation spectra is a great method that can provide an insight on the water environment inside the lignocellulosic matter and hints the influence of the microstructure and chemical composition on the hydrogen signal observed. Moreover, the influence of the two bound water components on dimensional properties has to be further investigated. According to Cox et al. (2010), only one component may contribute to wood swelling, whereas for Bonnet et al. (2017), the two components have an effect on the hydric strains.

The main purpose of this study is to analyse the effect of two aging methods on the hygrocopicity of wood material by using the 2D ^{1}H NMR relaxometry to evaluate the interactions between water and the cell wall's physical and chemical changes that may have occurred. A method to evaluate the 'true dry mass" of wood material is also proposed, enabling the calculation of the "true equilibrium moisture content" without the need of drying the samples at 103°C in an oven (which can lead to irreversible damages or misinterpretations). The evolutions/modifications are also discussed against hydric strains, as well as the possible contribution of the two water components on the volume deformation. A parallel objective of this work is to compare these changes between historical and modern oak woods.

Materials and Methods

Materials: The experiments were carried out on modern and historical oak wood samples to compare the effect of aging on two types of wood. The historical wood (350-year-old oak) was provided by Atelier Perrault, and comes from a wooden door's frame of an old building of the 17th century in Saint Georges street in Rennes, France. The historical oak wood has been subjected to natural aging. The modern oak wood was recently provided from a sawmill located in the North of France and may be considered without aging. Figure 1 provides an optical microscopy image of the transversal cross-section (plane RT) of both wood materials. The chemical composition and the proportion of the

different kinds of cells (vessel, fiber, parenchyma...) were not quantified in this study, but these images allowed confirming differences between these two oak materials.

Small specimens of approximately 1 cm^3 were prepared as 1 cm is the maximum height for optimal NMR measurements. This was done using a band saw and they were all clear from visible defects. They were sawn along the anisotropic directions (Longitudinal L, Radial R and Tangential T). All the samples were taken side by side, to minimize the variability between samples of the same type (modern wood or historical wood). The average density of all specimens was measured at 2% relative humidity (RH) and is 0.64 (±0.02) g cm^{-3} for modern oak wood and 0.47 (±0.02) g cm^{-3} for historical oak wood. The lower density of the historical wood is in accordance with the fact that there are more vessels.

All samples were subjected to a common cycle of adsorption-desorption to equalize their hydric history, using saturated salt solutions at 2% RH (silica gel) and 97% RH (potassium sulphate: K_2SO_4). They were kept in desiccators until constant mass (about one week). All the experiments were carried out at 20°C and on an adsorption cycle (starting from 2% RH) to avoid the influence of the hysteresis in the observed phenomena.

Aging protocols: Two aging methods were conducted, on the one hand repeated hydric cycles (considered as a "natural aging" method with gentle impact) and on the other hand mild thermal treatment (considered as an "accelerated aging" method). To compare the effect of these aging methods, the samples were all characterized through 2D ^{1}H NMR at equilibrium moisture content (Eq. 1):

$$EMC_{x\%RH} = \frac{M_{x\%RH} - M_{dry}}{M_{dry}} \times 100 \quad (1)$$

where $EMC_{x\%RH}$ is the equilibrium moisture content at x% RH [%], $M_{x\%RH}$ the mass of the equilibrated sample at x% RH [g] and M_{dry} the mass of dry sample [g].

129 Repeated hydric cycles consist in applying repeated cycles of adsorption and desorption to wood
130 specimens. In this study, three samples of modern wood and three samples of historical wood were
131 subjected successively to 2% RH and 97% RH using the method of saturated salt solutions to attain
132 EMC at room temperature (20°C). These hydric cycles were repeated during 6 months (corresponding
133 to a total of 12 cycles of adsorption-desorption) and samples were studied at 1, 3 and 6 months. In
134 order to study the evolution of the samples at each period, they were conditioned at 65% RH, 20°C
135 (using sodium nitrite ($NaNO_2$)) and analysed through ^{1}H NMR at EMC. In parallel, control samples
136 of modern and historical wood (three of each) were conditioned at 65% RH, 20°C, over the entire
137 period of the experiments. Deformation measurements and mass measurements were carried out
138 regularly on all samples to assess the EMC by weighing and the evolution of the hydric strains.

139 Thermal treatments (TT) were conducted in an oven at a temperature of 120°C (where RH is close to
140 0%) for three periods of time (24 hours, 3 days and 7 days). Prior to the TT, the initial state of each
141 specimen conditioned at 65% RH was characterized through 2D ^{1}H NMR at EMC at 20°C. After TT,
142 the specimens were again conditioned at 65% RH, 20°C for one week before a second ^{1}H NMR
143 analysis. This protocol allows to compare the EMC evolution for the same sample and to determine
144 the mass loss induced by the TT. Dimensions were also measured before and after treatment to assess
145 the change in volume deformation as this provides information on the stability of the wood. Three
146 specimens of each wood were considered for the 24 hours TT to take into account the variability of
147 wood material and to test the reproducibility and the repeatability of the used method. As the
148 variability was statistically tested with a Student T-test and showing significant changes after 24h TT,
149 only one specimen of each wood type was analysed for the 3 and 7 days TTs.
150
151 **NMR methods**: The samples were measured by 2D ^{1}H NMR and to do so they were inserted in
152 18mm NMR tubes. The RH was controlled with a saturated salt solution at 65% RH during the NMR
153 experiments (Bonnet et al. 2017, Fourmentin 2015) placed in a small container on the top of the NMR

tubes. As the temperature of the magnetic unit is 40°C, a cooling system is used to maintain the samples at 20°C (at the bottom of the NMR tubes). The temperature in the area of the saturated salt container (outside the instrument) corresponds to a temperature of 25±2°C (measured during NMR analysis). The theoretical variation of the saturated salt solution used is up to 2% decrease of RH at 30°C. To take into account possible variations on EMC, all samples were weighed before and after NMR measurements and the mean value of these two measurements was used to calculate the EMC. The difference in EMC calculated with the mass before NMR and the mass after NMR measurement was evaluated and resulted to be lower than 0.1%. Therefore, it is considered of a minor effect and does not affect the obtained results and interpretations. The device used was a BRUKER MINISPEC MQ20 spectrometer that operates at 0.5 T, corresponding to a resonance frequency of 20 MHz for ^{1}H.

The principle of NMR is based on the intrinsic nuclear spin that some atomic nuclei have (with an odd number of protons, neutrons, or both). When an atomic nucleus with a nonzero spin is placed in a magnetic field $\mathbf{B_0}$, the nuclear spin can be aligned in the same direction or in the opposite direction to the field. These two types of nuclear spin alignment are characterized by different energies, and their sum is called the magnetization ($\vec{M}$). When a second magnetic field (with a characteristic energy) $\mathbf{B_1}$, perpendicular to $\mathbf{B_0}$ is applied as a pulse, this magnetization is disturbed and the relaxation (=time needed for the magnetization to come back to its initial state) is characteristic of the atom and of the local environment (Kekkonen 2014). The two main relaxation times measured are: T_2, the spin−spin or transversal relaxation time and T_1, the spin−lattice or longitudinal relaxation time.

The Inversion Recovery (IR) sequence coupled with the Carr-Purcell-Meiboom-Gill (CPMG) sequence (Carr and Purcell 1954, Meiboom and Gill 1985) was used to obtain 2D NMR correlation spectra of the T_1 and the T_2 relaxation values. The calculation of T_1-T_2 correlation spectra from NMR data was performed with an in-house software, which essentially reproduces the 2D-Inverse Laplace Transform (ILT) algorithm of Song et al. (2002). For more details about this and about the acquisition

179 method and parameters, see Bonnet et al. 2017. The T_1-T_2 correlation spectra allow to show the NMR
180 signal as a function of the two relaxation times, T_1 and T_2, obtaining two different peaks for the
181 adsorbed water (which is not possible with 1D T_1 or T_2 spectra due to peak overlapping). The volume
182 under each peak of the 2D spectra is proportional to the amount of hydrogen (H) atoms. The T_1 and
183 T_2 values of each peak are determined by means of the coordinates of their respective maxima. 2D
184 spectra also give unambiguous access to T_1/T_2 ratios. The latter is characteristic of H atoms mobility
185 and confinement and greatly helps spectrum interpretation.
186
187 **Determination of EMC:** The moisture content can be calculated from the T_1-T_2 spectra, as the area
188 under the peaks is proportional to the amount of H atoms. Thus, the total moisture content can be
189 evaluated through NMR as the sum of the area under the two peaks corresponding to bound water.
190 In order to convert the NMR signal into a mass of adsorbed water, a standard curve is performed with
191 different quantities of water. The bound water mass ($M_{NMR,x\%RH}$) determined by ^{1}H NMR at x% RH
192 is defined by (Eq. 2):

$$q_{NMR,x\%RH} = \alpha . M_{NMR,x\%RH} \quad (2)$$

193 Where $q_{NMR,x\%RH}$ is the NMR signal intensity of peaks of interest and α the proportional coefficient
194 determined through the standard curve (in this study, α = 164.77 NMR signal/g of water).
195 To calculate $EMC_{NMR,x\%RH}$, it is necessary to determine the mass of the dry sample, M_{dry}. To avoid
196 irreversible structural damages or misinterpretations (in particular for thermal treatment), the studied
197 materials are never oven-dried at 103°C as usually done before heat treatments (Rajohnson 1996,
198 Obataya 2007, Candelier 2013). Therefore, ^{1}H NMR can be of good use to determine the "true dry
199 weight" of wood. Total mass of wood is weighed at EMC with a scale of precision ±0.0002g and the
200 amount of bound water at EMC is calculated through ^{1}H NMR as depicted previously. Thus, the mass
201 of dry wood M_{dry} [g] can be calculated as follows (Eq. 3):

$$M_{dry} = M_{w,x\%\mathrm{RH}} - M_{NMR,x\%\mathrm{RH}} \quad (3)$$

Where $M_{w,x\%RH}$ [g] is the total mass (dry wood and bound water) determined by weighing at x% RH (which corresponds to the average value of weighing before and after NMR experiments) and $M_{NMR,x\%RH}$ [g] is the bound water mass determined by NMR at x% RH. The moisture content determined through ^{1}H NMR measurements ($EMC_{NMR,x\%RH}$) is defined as $M_{NMR,x\%RH}$ divided by M_{dry}. The moisture content determined by weighing at x% RH ($EMC_{w,x\%RH}$) is defined as $M_{w,x\%RH} - M_{w,2\%RH}$ divided by $M_{w,2\%RH}$. These two moisture contents verify the following relationship (Eq. 4):

$$EMC_{NMR,x\%RH} = EMC_{w,x\%RH}\frac{M_{w,2\%RH}}{M_{dry}} + \frac{M_{w,2\%RH} - M_{dry}}{M_{dry}} \quad (4)$$

The obtained data for $EMC_{NMR,x\%RH}$, $EMC_{w,x\%RH}$, M_{dry} and $M_{w,2\%RH}$ are given in SI. Uncertainties on measurements for EMC are determined through the standard deviation values; they take into account the possible variability between samples' results and the precision of the balance (0.36% for the modern wood and 0.28% for the historical wood).

Volume measurements: In order to assess the changes in regard to the two aging methods, the samples' dimensions were measured with a Mitutoyo electronic calliper with a precision of ± 0.01mm. These measurements were performed at each step of the experiments for the three directions R, T and L allowing the calculation of the samples' volume: during the conditioning, at EMC, right before and after NMR measurements.

Measurements of the samples' dimensions allow to determine the deformation between two states, 2% RH and x% RH (with x=65% or 97% RH). Hydric strains at x% RH ($\varepsilon_{x\%}$) are related to the state

at 2% RH, as the volume of the dry wood was not experimentally measured as previously explained, according to (Eq. 5):

$$\varepsilon_{x\%} = \frac{V_{x\%RH} - V_{2\%RH}}{V_{2\%RH}} \times 100 \quad (5)$$

Where $V_{x\%RH}$ and $V_{2\%RH}$ are the volumes of a sample at x% RH and 2% RH respectively.

Note that the determination of the volume deformations was done using the state at 2% RH right before the conditioning at 65% RH for samples subjected to hydric cycles.

Uncertainties on deformation measurements are determined through standard deviation values; they take into account the possible variability between samples' results and the precision of the electronic calliper. For these experiments, the variability is about 0.39% for the modern wood and 0.30% for the historical wood. Also note that the EMC values for hydric strains may slightly differ from those during the NMR experiments due to possible variations of RH and temperature and because the dimension measurements are performed outside the desiccators.

Results and discussion

T_1-T_2 spectra and peak assignment: Figure 2 shows T_1-T_2 correlation spectra recorded from historical and modern oak wood samples (only one sample of each wood is represented here), before aging processes. Regardless of small differences in the shapes of the peaks observed in the cartographies, the global scheme is similar for both wood materials.

To interpret these spectra, it is necessary to understand the influence of water mobility and environment on the relaxation times T_1 and T_2. T_1 and T_2 depend on the local environment of the measured hydrogen atoms (H) (i.e. from water molecules and wood polymers in this work), that is to say: size of the molecules they are bound to, affinity with molecules interacting and pore size. T_2 relaxation time decreases as pore size is reduced. Moreover, T_2 will also be shortened when molecular tumbling (mobility) decreases. If H atoms are in molecules with restricted mobility due to viscosity,

243 or the interactions being in macromolecules or solid phase, T_2 values will decrease gradually
244 depending on the degree of this restriction. The case of T_1 is a bit more complicated than T_2 as it first
245 decreases when molecular tumbling decreases (from liquid phase) but it increases when molecular
246 tumbling is low (in gel and solid like molecules). Fortunately, T_1/T_2 ratios are characteristic of the
247 mobility of H atoms and greatly help spectrum interpretation. Depending on the value of these ratios,
248 water can be assigned to unconfined water, mobile water in a free or adsorbed state and bonded
249 immobile water molecules and solid macromolecules. It can be noticed that T_1/T_2 ratios lower than
250 one are physically not permitted (Bonnet et al. 2017).
251 Based on this knowledge, the peaks observed in the T_1-T_2 spectra can be identified based on analysis
252 previously done in Cox et al. (2010) and Bonnet et al. (2017). Peak A is labelled as liquid water in
253 the lumen as it has the highest T_1 and T_2 values and it is close to the T_1=T_2 line. In some spectra, this
254 peak is located slightly above the T_1=T_2 line, which certainly owes to the way the signal acquisition
255 was made. Indeed, the CPMG period of the NMR sequence was deliberately truncated after 12ms to
256 prevent excessive radio frequency (RF) power deposition in the sample and thus avoid heating the
257 sample. As a result, the measurement of T_2 value for peak A is not complete and lacks accuracy,
258 leading to a widening and 'mislocation' in T_2 direction. In our case, the amplitude of the peak is also
259 very low and it is therefore not of interest in this study. Peaks B and C correspond to bound water in
260 two specific and distinct water reservoirs in the wood cell walls. The T_1/T_2 ratio is higher for peak B
261 than for peak C, indicating a more restricted molecular motion in compartment B and thus more
262 strongly bonded water molecules in that compartment. In contrary, the low T_1/T_2 ratio for peak C
263 indicates less restricted molecular motion and less strongly bonded water molecules. In some spectra,
264 peak C seems to split into two peaks, one with lower T_1 and T_2 values than the other peak but having
265 almost the same T_1/T_2 ratio. This could be interpreted as two types of C-water with small differences
266 on their environment (e.g. surface-to-volume ratio). In general, the peak with higher T_2 and T_1 values
267 is most intense, but in few cases, it is the other one showing higher amplitude. Thus, for easier

268 interpretation, the peak taken into account for the calculation of T_1 and T_2 values of peak C is always
269 the one with higher T_1 and T_2 values. It would be interesting to understand the nature of this splitting
270 but it is out of scope of this work. Finally, peak D represents H atoms from the wood polymers since
271 the T_2 value relaxes very fast (in the order of µs).
272 Among the recent results, Bonnet et al (2017) have proposed to relate the two components B and C
273 to the structure of the S2 layer of the cell wall, because this layer may explain the mechanical
274 properties and especially the hydric strains. Based on a schematic structure of the S2 layer inspired
275 by Boyd (1982) and Salmén and Burgert (2009), it has been explained that the population of water
276 from component B (strongly bonded) may be located in the macrofibrils composed mainly of
277 microfibrils of crystalline and amorphous cellulose embedded in a matrix of hemicelluloses
278 (primarily glucomannan for softwoods). While the population of water from component C (weakly
279 bonded) may be in a lignin and hemicelluloses (xylan) matrix corresponding to the intra-macrofibril
280 region. The attribution of the two bound water components B and C to these two regions is related to
281 the fact that water affinity is higher in the region composed of cellulose and hemicelluloses than in
282 the region composed of lignin and hemicelluloses. However, the proportion of polymers differ
283 between hardwoods and softwoods (Chaouch et al. 2010). Hardwoods contain mainly glucuronoxylan
284 and low amount of glucomannan. Thus, for our studied materials, it can be suggested that xylan
285 (glucuronoxylan) may be present in the two regions.
286
287 **NMR results for samples at the initial state:** Table 1 presents the average results obtained from
288 NMR measurements on the control samples of hydric cycles and on the samples at the initial state
289 before TT. EMC values (deduced from the sum of peaks B and C) are the same order of magnitude
290 for both woods. Furthermore, peak B reveals a higher moisture content than peak C for both woods,
291 meaning that this compartment contains more adsorbed water than the other one. Compartment C

292 shows higher water content for the historical wood than for the modern wood, while there is less
293 water in compartment B for historical wood.
294 These differences in terms of relative moisture content in B and C could provide new insights in terms
295 of evolution in the structure and composition of the wood cell wall. The higher moisture content in
296 compartment C of the historical wood appears to indicate a higher amount of available adsorption
297 sites in that region compared to the modern wood. The higher content of adsorption sites could be
298 due to an evolution of the polymeric structure such as a change in the polymers conformation. Indeed,
299 the lignin undergoes structural changes due to oxidation during aging but, as shown in Kranitz 2014,
300 the absolute amount remains the same. Therefore, these structural changes in the lignin could free
301 some previously inaccessible hydroxyl sites for water adsorption.
302 NMR results give an additional indication in favor of the hypothesis made on the local environment
303 of water in compartment B, which is mainly composed of cellulose and hemicelluloses. As mentioned
304 earlier, the hemicelluloses are the first polymers to degrade during wood aging and a decrease in
305 amorphous cellulose is observed in naturally aged woods (Kranitz 2014), thus leading to a decreased
306 number of adsorption sites and therefore lower moisture content in that region for historical wood
307 compared to the modern wood. However, it may be difficult to quantitatively compare these two oak
308 wood types without chemical characterization. This is a common issue found when historical and
309 modern wood are to be compared, as the composition and proportion of polymers in the cell wall
310 before aging are not known. The environmental conditions and geographical location are also a source
311 of variability in the wood development and evolution. Thus, to improve our understanding of the
312 relative differences on the amounts of B and C ‘water’ between historical and modern oak wood, a
313 detailed chemical analysis could be useful (e.g. characterization and quantification of wood polymers)
314 in future works.
315

316 **NMR results for repeated hydric cycles:** Table 2 presents the moisture content measured during
317 the repeated hydric cycles as well as the characteristic relaxation times T_1 and T_2 for all samples. A
318 graphical representation of the evolution in total moisture content is also presented in Figure 3.
319 First observation shows that hydric cycles did not really affect the adsorption behaviour of the
320 samples, meaning that no significant increase or decrease in EMC is observed in regards to the
321 standard deviation values. A paired Student T-test was performed on all the moisture content
322 measures ($EMC_{NMR,65\%RH}(B+C)$, $EMC_{NMR,65\%RH}(B)$ and $EMC_{NMR,65\%RH}(C)$) showing no significant
323 evolution of the EMC (p-values > 0.05) along the 6 months of repeated hydric cycles. Moreover, the
324 evolution of the T_1/T_2 ratio is globally constant. This indicates no change in the mobility of water
325 pools, thus no change in the polymeric structure of the cell wall, i.e. no change in the hygroscopicity
326 of the wood material. Such results were expected since the room temperature and humidity are fixed
327 and controlled along the experiment, which is not the case in natural conditions of aging. Furthermore,
328 mass of samples was recorded during the cycles and permits to estimate the mass loss through the 6
329 months cycles, showing no significant mass loss through the whole experiment period.
330 In conclusion, although these repeated hydric loads may have an influence on the hydric properties
331 over the long term, we suppose that the duration of tests is not sufficient to induce a significant effect
332 on the hygroscopic properties. This result will be discussed with the hydric deformation
333 measurements below.
334
335 **NMR results for moderate heat treatment:** NMR data are presented in Table 3 and a graphical
336 representation of the evolution in total moisture content before and after the heat treatments is
337 presented in Figure 3.
338 A noticeable loss in total $EMC_{NMR,65\%RH}(B+C)$ is observed for both modern and historical wood
339 samples and the longer the treatment, the higher the loss in hygroscopicity, as expected. Thermal
340 treatments also show a total higher effect on the historical wood than on modern wood. There is a

341 higher EMC loss for historical wood the longer the treatment time (13% for modern wood against
342 19% for historical wood, in average of the 72 h and 168 h TT). The loss of water in compartments B
343 and C can be calculated separately, showing for the 24 h TT a higher percentage of water loss in peak
344 C (18.0%) than peak B (6.9%) for historical wood. While it seems to be the contrary for modern oak
345 wood, with higher loss in compartment B (11.5%) than C (9.9%). The same conclusions were
346 obtained for the 72 h and 168 h TTs.
347 A Student T-test was performed on these percentages of loss in EMC for the 24 h TT, showing no
348 significant difference between the loss in $\mathrm{EMC}_{\mathrm{NMR,65\%RH}}(\mathrm{B})$ and $\mathrm{EMC}_{\mathrm{NMR,65\%RH}}(\mathrm{C})$ for modern wood.
349 For historical wood, the statistical tests confirmed a significant difference between peaks B and C,
350 with a higher loss for $\mathrm{EMC}_{\mathrm{NMR,65\%RH}}(\mathrm{C})$. As mentioned previously, the strongly bound water
351 (component B) may be located in the macrofibrils (cellulose-glucuronoxylan-glucomannan matrix) -
352 and the weakly bound water in the lignin-glucuronoxylan matrix (component C). It is suggested in
353 Salmén and Burguert (2009) that there might be a highly acetylated xylan which is closely associated
354 to a less condensed type of lignin, whereas low substituted xylans are associated with cellulose and a
355 condensed type of lignin. It can be noticed that xylan units of hemicelluloses in hardwoods are
356 generally strongly acetylated, generating a higher sensitivity of these materials to thermal treatments,
357 as the xylan units could lead to higher kinetic of thermo-degradation in hardwoods (Chaouch et al.
358 2010). Therefore, one could assume that the highly acetylated xylan are linked with the component
359 C, while the low-substituted xylan is linked to the component B. These associations could be of major
360 importance in regard of the selective evolution of wood adsorption.
361 For the historical wood, it seems that the dry mass loss (Table 4) is greater with treatment time.
362 Indeed, the dry mass loss for 72 and 168 h TTs was higher than for the 24 h treatment, but as only
363 one sample was used for these two durations, observations are mostly qualitative. For the modern
364 wood, the same observation was made except for the 168 h TT that seems to be an outlier due to its
365 low value, but which is due to the fact that it is the dry mass loss of a single sample. Recent tests

366 confirmed an increased dry mass loss with treatment time for modern wood, up to 2.3%. Nevertheless,
367 these percentages of dry mass loss are quite low and according to Kollmann and Fengel (1965) and
368 Esteves and Pereira (2008) wood degradation begins only at 130-150°C for oak wood. Thus, by
369 heating at 120°C, there should be no degradation of polymers and the dry mass loss observed may be
370 due to a loss of extractives during heat treatment as discussed in Esteves and Pereira 2008.
371 In our case, the extractives degradation cannot fully explain the loss in EMC observed after TT,
372 knowing that not all the extractives are volatile (Hillis 1971, Esteves and Pereira 2008, Jankowska et
373 al. 2017). Indeed, the T_1-T_2 correlation spectra reveal a global increase of the T_1/T_2 ratio after thermal
374 treatments (Table 3), indicating that there are stronger bonds between adsorption sites and water
375 molecules. The ratio increase also indicates the confinement of the H atoms detected. The evolution
376 of H atoms mobility could be due to a restricted space between polymers therefore changing the local
377 environment of H atoms. When wood is oven-dried in a dry atmosphere, various chemical changes
378 take place producing a "shrunken" state for which the intermolecular space is minimized (Obataya
379 2007). Thus, when wood is reconditioned at 65% RH, the restricted intermolecular space will not
380 allow the adsorption of the water molecules in several layers as it used to before TT. This hypothesis
381 can also be interpreted by looking at the evolution of peak C for instance (Figure 4), which can be
382 divided into two parts to highlight two populations of water. The lower part corresponds to the least
383 mobile H atoms and therefore the most strongly linked water molecules (directly linked to the
384 adsorption sites). The upper part corresponds to the most mobile H atoms and therefore the least
385 strongly linked water molecules (upper additional layers of adsorbed water) (see Figure 4b).
386 Following the TT, peak C is shifted downward (T_2 decreases and T_1 increases) showing a larger
387 population of H atoms more strongly bound to the polymeric matrix, but there has been a loss of the
388 less strongly bound H population. Consequently, there is a loss of additional layers of adsorbed water
389 molecules due to the smaller intermolecular space following TT. Note that this observation is similar

390 for peak B. The shrinking of the polymeric matrix could be a plausible explanation for the increase
391 in the confinement of bound water molecules and therefore for the decrease in water adsorption.
392
393 **Discussion in relation with deformation:** The hydric strains of studied materials either subjected to
394 repeated hydric cycles or to thermal treatments are given in Figure 5 and are compared to those
395 without aging (control samples and samples at the initial state). They are expressed as a function of
396 total EMC ($EMC_{NMR,65\%HR}(B + C)$) determined by ^{1}H NMR from the components B and C. Note
397 that, if the hydric strains (related to the state at 2% RH) are plotted against EMC (related to dry mass)
398 it is observed that the hydric strains for modern and historical wood materials vary linearly with the
399 moisture content, as expected for wood materials (see SI for more details). The slope β of the obtained
400 linear law expressed as a function of EMC is 0.50 for modern wood 0.45 for historical wood. It can
401 be noticed that the value of the slope is related to the density of the studied materials (Bonnet 2017)
402 and the slope β decreases with decreasing density. According to the above results (see Table 2 and
403 Table 3), the densities of the samples after "natural" or "artificial" aging do not significantly vary, so
404 the slope remains the same after aging. Thanks to this linear law between hydric strains and EMC, it
405 is possible to discuss the influence of each bound water compartments (B or C) on the decrease of
406 volume deformation. This evolution is related to the decrease of EMC(B) and EMC(C) which is
407 related to the decrease of EMC(B+C) for samples subjected to aging, see SI for more details.
408 The hydric strains for samples subjected to repeated hydric cycles seem to be "globally" stable
409 through the 6 months cycles (Figure 5) for modern and historical wood materials. This is in coherence
410 with a "globally" stable EMC. Note that the hydric strains of the samples at one month are higher
411 than those of the control samples, in coherence with higher EMC (Table 2). Between 1 month and 6
412 months cycles there is surprisingly a slight decrease of the volume deformations with no decrease of
413 the EMC. Further studies are necessary to confirm these unexpected results (at other durations).
414 Moreover, it seems to be more important for modern wood than for historical wood (Figure 5) in

coherence with the fact that the hemicelluloses are supposed to be mostly degraded in historical wood (Kranitz 2014, Obataya 2007), thus leaving a material more stable in terms of volume deformation. Concerning the samples subjected to thermal treatments, the hydric strains significantly decreased after TT and with treatment duration. However, the effect seems to be weaker for the modern wood than for historical wood. The contribution of each component (B or C) on the hydric strains is not the same for both studied materials. For historical wood material, the contribution of compartment C on volume deformation decreases with treatment time while the contribution of component B increases (see Table 5). Furthermore, the component C contributes the most in the loss of volume deformation for historical wood, which means that for higher treatment times, the lignin-xylan matrix might undergoes some chemical changes that reduces the hygroscopicity of the wood cell wall. As for the modern wood, inverse phenomena was observed with a decrease in contribution of component B in the loss of volume deformation, while component C seems to increase. Nevertheless, the contribution of compartment C in modern wood presents higher percentage meaning that it has a higher influence on the decrease in volume deformation.

To conclude, the use of NMR by quantifying the two components B and C and relating them to the possible modification of hygroscopicity due to aging, appears to be an available and accurate method to evaluate the decrease of hydric strains. Furthermore, these results confirm that the two components B and C have an effect on hydric deformation, especially for thermal treatments.

Conclusions

This study shows the potential of the 2D ^{1}H NMR correlation spectra to study modifications in wood hygroscopicity by being the sole technique able to quantify two types of adsorbed water in two

different chemical environments in the wood cell walls. This method also permits to determine the moisture content of wood without the necessity to oven-dry the wood material.

Two aging methods have been conducted on two oak wood materials (modern and historical wood), on the one hand "natural" aging with repeated hydric cycles and on the other hand "artificial" aging with mild thermal treatment. Results show that the duration of the "natural" aging seems to be not sufficient to induce evolution on the hygroscopic properties, but unexpected results over time were observed for the hydric strains. More investigations are necessary, especially with other durations. Concerning "artificial" aging, a clear reduction in total moisture content was observed after heat treatment and reconditioning at 65% RH for the two types of oak wood, accompanied with low dry mass loss. The observed decrease of water content is in accordance with the decrease of the swelling strains between 2% RH and 65% RH. Moreover, T_1-T_2 NMR experiments allow us to measure the effect of heat treatment for the two types of adsorbed water by showing a higher percentage of water loss in one compartment than in the other for the historical oak wood. The reason of this selective loss of water adsorption can be explained in relation with the chemical composition of the studied materials. The global decrease of EMC is the result of the loss of extractives but also of structural modifications such as restricted space between polymers leading to a decrease of adsorbed water layers. This is shown by the increase of the T_1/T_2 ratio which indicates a decrease on the averaged mobility of H atoms for each water pool after TT and stronger interactions (bonds) between wood and adsorbed water molecules. All these results could be completed with ^{13}C NMR or IR investigation to determine the changes that occurred in wood polymers more precisely.

Acknowledgments

The I-Site Future (Champs-sur-Marne, France) for its financial support and Atelier Perrault (Nantes, France) for providing aged wood are acknowledged.

References

Araujo, C.D., Avramidis, S., MacKay, A.L. (1994). Behaviour of solid wood and bound water as a function of moisture content: a proton magnetic resonance study. Holzforschung 48:69-74.

Beck, G., Thybring, E.E., Thygesen, L.G., Hill, C. (2018). Characterization of moisture in acetylated and propionylated radiata pine using low-field nuclear magnetic resonance (LFNMR) relaxometry. Holzforschung 72(3), pp. 225-233

Bonnet, M., Courtier-Murias, D., Faure, P., Rodts, S., & Care, S. (2017). NMR determination of sorption isotherms in earlywood and latewood of Douglas fir. Identification of bound water components related to their local environment. Holzforschung, 71(6), 481-490.

Bonnet, M. (2017). Analyse multi-échelle du comportement hygromécanique du bois: Mise en évidence par relaxométrie du proton et mesures de champs volumiques de l'influence de l'hétérogénéité au sein du cerne (Doctoral dissertation, Université Paris-Est, France). In French.

Boyd, J.D. (1982). An anatomical explanation for visco-elastic and mechano-sorptive creep in wood, and effects of loading rate on stregth. In: New Perspectives in Wood Anatomy, Eds. Martinus Nijhoff/Dr. W. Junk Publishers, La Hague. pp. 171–222.

Candelier, K. (2013). Caractérisation des transformations physico-chimiques intervenant lors de la thermodégradation du bois. Influence de l'intensité de traitement, de l'essence et de l'atmosphère (Doctoral dissertation, Université de Lorraine). In French.

Candelier, K., Thevenon, M. F., Petrissans, A., Dumarcay, S., Gerardin, P., & Petrissans, M. (2016). Control of wood thermal treatment and its effects on decay resistance: a review. Annals of Forest Science, 73(3), 571-583.

Carr, H. Y., & Purcell, E. M. (1954). Effects of diffusion on free precession in nuclear magnetic resonance experiments. Physical review, 94(3), 630.

Chaouch, M., Pétrissans, M., Pétrissans, A., & Gérardin, P. (2010). Use of wood elemental composition to predict heat treatment intensity and decay resistance of different softwood and hardwood species. Polymer Degradation and Stability, 95(12), 2255-2259.

Chaouch, M. (2011). Effet de l'intensité du traitement sur la composition élémentaire et la durabilité du bois traité thermiquement: développement d'un marqueur de prédiction de la résistance aux champignons basidiomycètes (Doctoral dissertation, Nancy 1). In French.

Cox, J., McDonald, P. J., & Gardiner, B. A. (2010). A study of water exchange in wood by means of 2D NMR relaxation correlation and exchange. Holzforschung, 64(2), 259-266

Endo, K., Obataya, E., Zeniya, N., & Matsuo, M. (2016). Effects of heating humidity on the physical properties of hydrothermally treated spruce wood. Wood science and technology, 50(6), 1161-1179.

Épaud F. (2007). De la charpente romane à la charpente gothique en Normandie. Évolution des techniques et des structures de charpenterie aux XIIe-XIIIe siècles, Caen, Publications du CRAHM (« Archéologie médiévale »), 624 p. In French.

Esteves, B., & Pereira, H. (2008). Wood modification by heat treatment: A review. BioResources, 4(1), 370-404.

Fayolle, B., & Verdu, J. (2005). Vieillissement physique des matériaux polymères. Ed. Techniques Ingénieur. In French.

Fourmentin, M. (2015) Impact de la répartition et des transferts d'eau sur les propriétés des matériaux de construction à base de chaux formulées. PhD thesis: Université Paris-Est, France. In French.

Fredriksson M. and Garbrecht Thygesen L. (2017), The states of water in Norway spruce (Picea abies (L.) Karst.) studied by low-field nuclear magnetic resonance (LFNMR) relaxometry: assignment of free-water populations based on quantitative wood anatomy. Holzforshung, 71(1): 77–90

Froidevaux, J. (2012). Wood and paint layers aging and risk analysis of ancient panel painting (Doctoral dissertation, Université Montpellier II-Sciences et Techniques du Languedoc).

Gauvin, C. (2015). Étude expérimentale et numérique du comportement hygromécanique d'un panneau de bois. Application à la conservation des tableaux peints sur bois du patrimoine (Doctoral dissertation, University of Montpellier, France). In French.

Hahn, E. L. (1949). An accurate nuclear magnetic resonance method for measuring spin-lattice relaxation times. Physical Review, 76(1), 145.

Hill, C. A. S. (2006). Wood modification: chemical, thermal and other processes. John Wiley & Sons.

Hillis, W. E. (1971). Distribution, properties and formation of some wood extractives. Wood Science and technology, 5(4), 272-289.

Inari, G. N., Pétrissans, M., Pétrissans, A., & Gérardin, P. (2009). Elemental composition of wood as a potential marker to evaluate heat treatment intensity. Polymer Degradation and Stability, 94(3), 365-368.

Jankowska, A., Drożdżek, M., Sarnowski, P., and Horodeński, J. (2017). "Effect of extractives on the equilibrium moisture content and shrinkage of selected tropical wood species," BioRes. 12(1), 597-607.

Kekkonen, P., (2014). Characterization of thermally modified wood by NMR spectroscopy: microstructure and moisture components. (Academic dissertation, University of Oulu, Finland).

Kollmann, F., & Fengel, D. (1965). Changes in chemical composition of wood by thermal treatment. Holz als Roh-und Werkstoff, 23(12), 461.

Kránitz, K., Sonderegger, W., Bues, C. T., & Niemz, P. (2016). Effects of aging on wood: a literature review. Wood science and technology, 50(1), 7-22.

Labbé, N.; Jéso, B.D.; Lartigue, J.-C.; Daudé, G.; Pétraud, M.; Ratier, M.; Labbé, N.; Jéso, B.D.; Lartigue, J.C.; Daudé, G. (2002). Moisture Content and Extractive Materials in Maritime Pine Wood by Low Field ^{1}H NMR. Holzforschung, 56, 25–31.

Meiboom, S. and Gill, D. (1958). Modified Spin-Echo Method for Measuring Nuclear Relaxation Times, Rev. Sci. Instrum., 29, 688–691, doi:10.1063/1.1716296.

Menon, R.S.; Mackay, A.L.; Hailey, J.R.T.; Bloom, M.; Burgess, A.E.; Swanson, J.S. (1987). An NMR determination of the physiological water distribution in wood during drying. J. Appl. Polym. Sci., 33, 1141–1155.

Murata, K., Watanabe, Y., & Nakano, T. (2013). Effect of thermal treatment on fracture properties and adsorption properties of spruce wood. Materials, 6(9), 4186-4197

Obataya, E. (2007). Effects of ageing and heating on the mechanical properties of wood. In Wood Science for Conservation of Cultural Heritage, Florence 2007: Proceedings of the International Conference Hld by Cost Action IE0601 in Florence (Italy), 8-10 November 2007 (pp. 1000-1008). Firenze University Press.

Rajohnson, J. R. (1996). Etude expérimentale et modélisation du traitement thermique de rétification du bois massif sous gaz convectif en vue d'améliorer ses propriétés physico-chimiques (Doctoral dissertation, Ecole Nationale Supérieure des Mines de Saint-Etienne). In French.

Rautkari, L., Hill, C. A., Curling, S., Jalaludin, Z., & Ormondroyd, G. (2013). What is the role of the accessibility of wood hydroxyl groups in controlling moisture content?. Journal of Materials Science, 48(18), 6352-6356.

Salmén, L., Burgert I. (2009). Cell wall features with regard to mechanical performance. A review. Holzforschung 63:121–129.

Sandberg, D., Haller, P., & Navi, P. (2013). Thermo-hydro and thermo-hydro-mechanical wood processing: An opportunity for future environmentally friendly wood products. Wood Material Science & Engineering, 8(1), 64-88.

Song, Y.Q., Venkataramanan, L., Hürlimann, M.D., Flaum, M., Frulla, P., Straley, C. (2002). T1-T2 correlation spectra obtained using a fast two-dimensional Laplace inversion. J. Magn. Reson. 154:261–268.

559 Tjeerdsma, B. F., Boonstra, M., Pizzi, A., Tekely, P., & Militz, H. (1998). Characterisation of
560 thermally modified wood: molecular reasons for wood performance improvement. Holz als
561 Roh-und Werkstoff, 56(3), 149.
562 Wentzel, M., Altgen, M., & Militz, H. (2018). Analyzing reversible changes in hygroscopicity of
563 thermally modified eucalypt wood from open and closed reactor systems. Wood Science and
564 Technology, 1-19.
565
566

TABLES

Table 1: Density [g/cm^3] and 2D ^{1}H NMR results ($EMC_{NMR,65\%}$ noted B+C [%] and the ratio T_1/T_2 [-]) for the specimens at 65% RH (samples without hydric or thermal loadings). Average values (mean) and standard deviation (SD) are given.

	Modern wood Mean (SD)	Historical wood Mean (SD)
Density g/cm^3	0.67 (0.02)	0.50 (0.02)
B+C [%]	12.10 (0.36)	11.51 (0.29)
B [%]	9.24 (0.34)	7.36 (0.39)
T1/T2	88.39 (3.46)	76.06 (7.39)
C [%]	2.86 (0.20)	4.15 (0.58)
T1/T2	3.34 (0.12)	3.83 (0.67)

Table 2: Density [g/cm^3] and 2D ^{1}H NMR results ($EMC_{NMR,65\%}$ noted B+C [%] and the ratio T_1/T_2 [-]) of the specimens subjected to repeated hydric cycles. Average values (mean) and standard deviation (SD) are given.

	Modern wood Mean (SD)				Historical wood Mean (SD)			
	Control samples	1 month	3 months	6 months	Control samples	1 month	3 months	6 months
Density g/cm^3	0.65 (0.04)	0.66 (0.02)	0.65 (0.02)	0.64 (0.02)	0.49 (0.02)	0.48 (0.01)	0.47 (0.01)	0.47 (0.01)
B+C [%]	12.08 (0.11)	12.46 (0.04)	12.45 (0.07)	12.47 (0.02)	11.59 (0.35)	11.85 (0.23)	11.90 (0.35)	12.23 (0.36)
B [%]	9.16 (0.13)	9.20 (0.18)	9.28 (0.09)	9.36 (0.12)	7.46 (0.43)	7.83 (0.50)	7.89 (0.79)	7.12 (1.11)
T1/T2	91.16 (0.00)	82.90 (5.43)	87.84 (5.75)	84.52 (5.75)	84.61 (7.37)	81.20 (0.00)	81.29 (4.70)	75.20 (2.49)
C [%]	2.92 (0.23)	3.27 (0.15)	3.17 (0.08)	3.11 (0.10)	4.13 (0.77)	4.02 (0.35)	4.01 (0.65)	5.11 (0.99)
T1/T2	3.37 (0.20)	3.80 (0.39)	4.17 (0.28)	3.94 (0.27)	4.24 (0.97)	4.10 (0.37)	4.19 (0.52)	4.03 (0.47)

Table 3: Density [g/cm^3] and 2D ^{1}H NMR results ($EMC_{NMR,65\%}$ noted B+C [%] and the ratio T_1/T_2 [-]) for the specimens subjected to moderate heat treatment. Average values (mean) and standard deviation (SD) are given.

	Modern wood Mean (SD)			Historical wood Mean (SD)		
Time of treatment	24h	72h	168h	24h	72h	168h
Density [g/cm^3]	0.68 (0.01)	0.65	0.65	0.50 (0.02)	0.48	0.46
B+C [%]	10.90 (0.21)	10.04	10.20	10.34 (0.32)	9.02	8.97
B [%]	8.34 (0.20)	7.69	8.06	6.82 (0.46)	6.34	6.30
T1/T2 [-]	111.73 (5.27)	128.99	128.99	100.38 (9.85)	114.90	128.99
C [%]	2.57 (0.16)	2.35	2.14	3.52 (0.61)	2.68	2.67
T1/T2 [-]	4.05 (0.18)	4.25	3.78	4.41 (0.29)	3.57	4.01

Table 4: Mass of specimens [g] before and after heat treatments and the relative mass loss [%]. *this value may be an outlier.

Thermal Treatment time	Modern wood Mean (SD)			Historical wood Mean (SD)		
	Before treatment [g]	After treatment [g]	Relative % mass loss	Before treatment [g]	After treatment [g]	Relative % mass loss
24h	0.5731 (0.06)	0.5715 (0.06)	0.27 (0.19)	0.4313 (0.06)	0.4292 (0.05)	0.46 (0.54)
72h	0.5781	0.5746	0.61	0.4303	0.4265	0.87
168h	0.4634	0.4623	0.23*	0.3874	0.3783	2.36

Table 5: Contribution of components B and C [%] on the variation of hydric deformation at 65%HR before and after aging. This contribution is given by $\Delta EMC(B \text{ or } C)$ divided by $\Delta EMC(B + C)$.

Thermal treatment time	Modern wood		Historical wood	
	B [%]	C [%]	B [%]	C [%]
24h	78.6	21.4	39.3	60.7
72h	70.8	29.2	41.3	58.7
168h	55.2	44.8	51.4	48.5

591 **FIGURES**

592

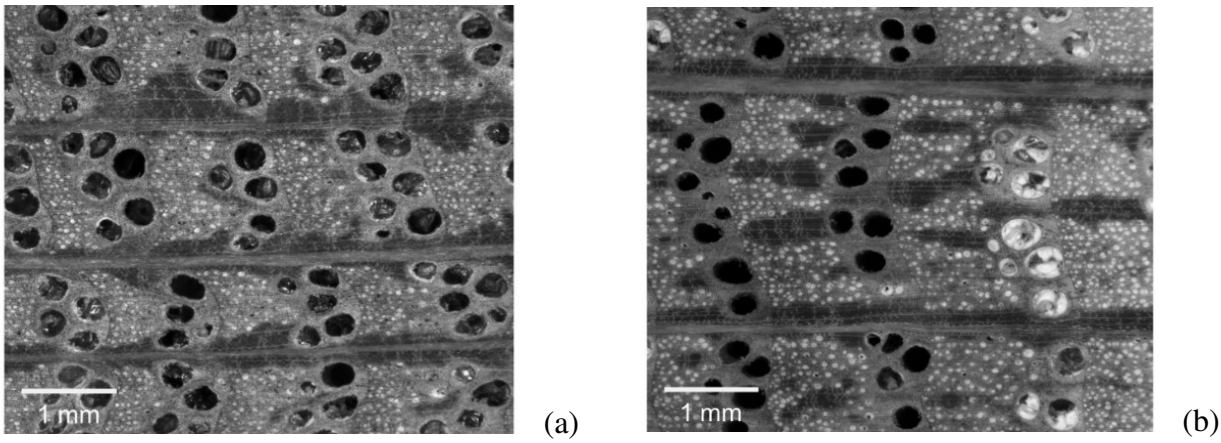

593 **Figure 1:** Optical microscopy image of transversal cross-section of the historical oak wood (a) and
594 the modern oak wood (b). Fibers were possibly filled with wood powder during the polishing (in
595 white in the fibers).
596

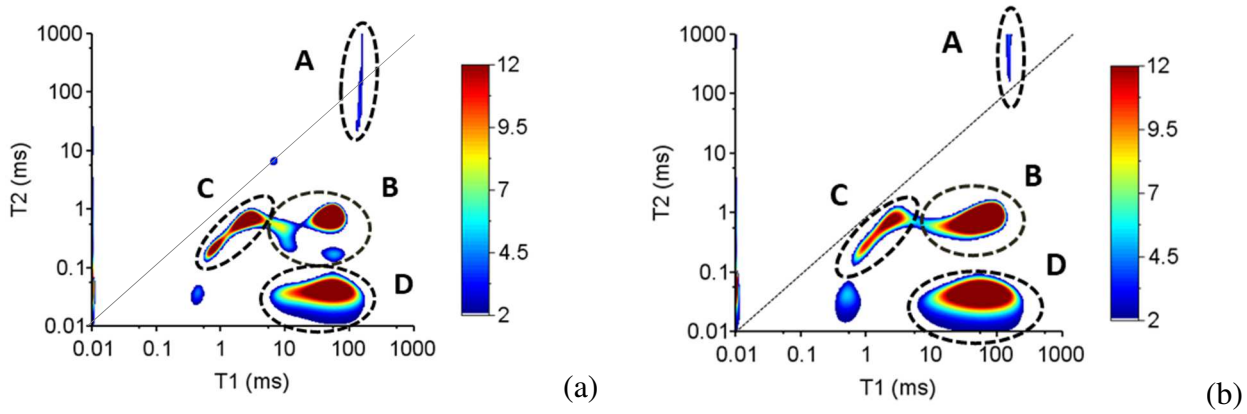

597 **Figure 2:** T_1-T_2 correlation spectra of the historical oak wood (a) and the modern oak wood (b) at
598 the initial state before aging at 65% RH, 20°C. Diagonal lines correspond to T_1=T_2.
599

600

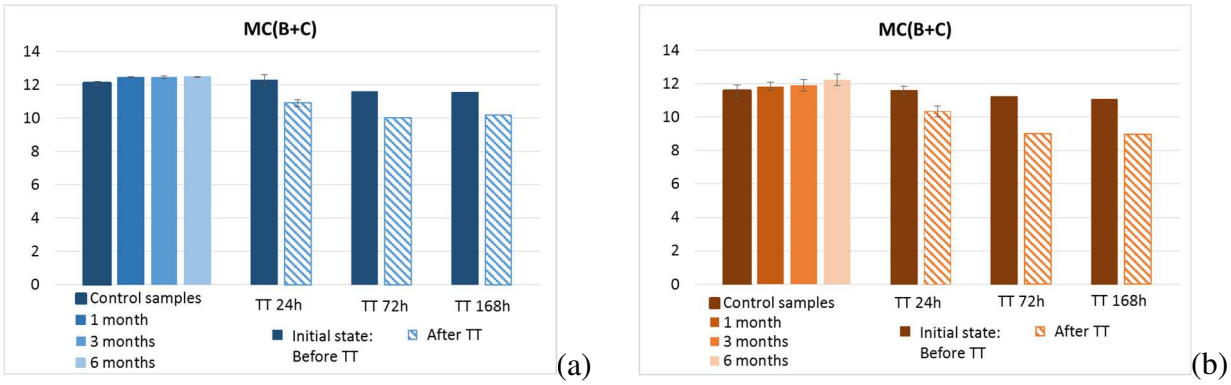

Figure 3: Evolution of the total moisture content $EMC_{NMR,65\%RH}$(B+C) noted MC(B+C) [%] for (a) modern and (b) historical wood samples subjected to repeated hydric cycles and moderate thermal treatment.

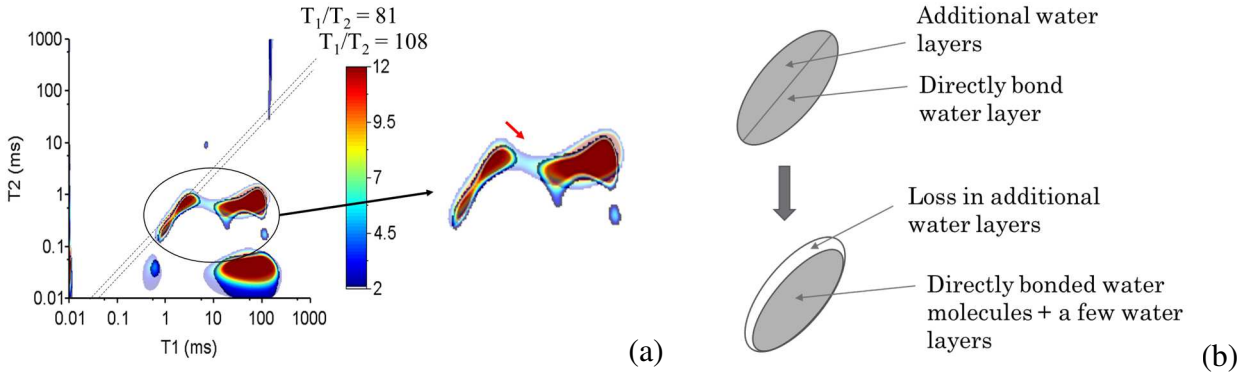

Figure 4: (a) Superposition of two T_1-T_2 correlation spectra of the same modern wood sample before (in transparency) and after (in bright colour) heat treatment. (b) Schematic representation of the evolution of "peak C" following a thermal treatment.

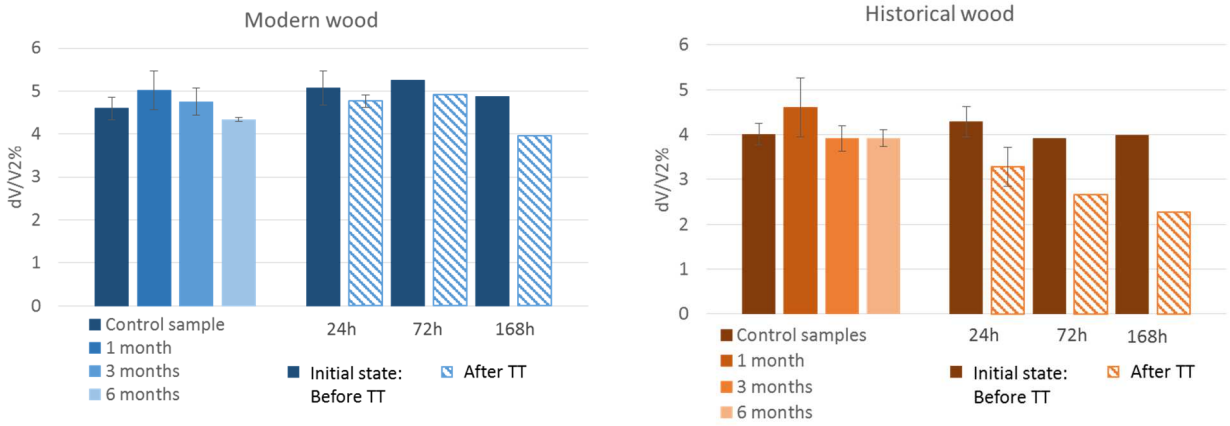

Figure 5: Volume deformations of samples (according to Eq. 5) without aging and through the 6 months repeated hydric cycles and for the thermal treatments.